

# Role of TiO<sub>2</sub> Surface Passivation on Improving the Performance of p-InP Photocathodes

Yongjing Lin,<sup>†,‡,⊥</sup> Rehan Kapadia,<sup>†,⊥</sup> Jinhui Yang,<sup>‡,⊥</sup> Maxwell Zheng,<sup>†,⊥</sup> Kevin Chen,<sup>†,⊥</sup> Mark Hettick,<sup>†,‡,⊥</sup> Xingtian Yin,<sup>†,⊥</sup> Corsin Battaglia,<sup>†,⊥</sup> Ian D. Sharp,<sup>‡,⊥,§</sup> Joel W. Ager,<sup>\*,‡,⊥</sup> and Ali Javey<sup>\*,†,‡,⊥</sup>

<sup>†</sup>Electrical Engineering and Computer Sciences, University of California, Berkeley, California 94720, United States

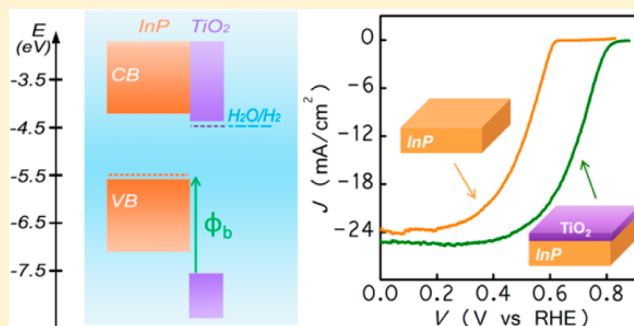
<sup>‡</sup>Joint Center for Artificial Photosynthesis, Lawrence Berkeley National Laboratory, Berkeley, California 94720, United States

<sup>⊥</sup>Materials Sciences Division, Lawrence Berkeley National Laboratory, Berkeley, California 94720, United States

<sup>§</sup>Physical Biosciences Division, Lawrence Berkeley National Laboratory, Berkeley, California 94720, United States

## S Supporting Information

**ABSTRACT:** The role of TiO<sub>2</sub> thin films deposited by atomic layer deposition on p-InP photocathodes used for solar hydrogen generation was examined. It was found that, in addition to its previously reported corrosion protection role, the large valence band offset between TiO<sub>2</sub> and InP creates an energy barrier for holes reaching the surface. Also, the conduction band of TiO<sub>2</sub> is well-aligned with that of InP. The combination of these two effects creates an electron-selective contact with low interface recombination. Under simulated solar illumination in HClO<sub>4</sub> aqueous electrolyte, an onset potential of >800 mV vs RHE was achieved, which is the highest yet reported for an InP photocathode.



## INTRODUCTION

Photosynthesis is a process adopted by nature to harvest solar energy by direct conversion into chemical energy.<sup>1</sup> Replicating this natural process more efficiently is a promising means to tackle the energy challenge and has received extensive scientific attention.<sup>2–6</sup> Specifically, artificial photosynthesis would enable the production of hydrogen from water reduction or liquid fuels, such as methanol, from carbon dioxide reduction.<sup>7–10</sup> Development of efficient and stable photocathodes, which use photogenerated minority carrier electrons to either reduce water or carbon dioxide, are essential to achieving this goal.

A number of semiconductors have been reported as promising photocathodes for water reduction, including Si,<sup>11–13</sup> InP,<sup>14–18</sup> WSe<sub>2</sub>,<sup>19</sup> Cu<sub>2</sub>O,<sup>20–23</sup> GaP,<sup>24</sup> and CuInGaSe<sub>2</sub>.<sup>25</sup> The energy conversion efficiency of some of these photocathodes has exceeded 10%.<sup>11,14,15</sup> To enhance stability, metal oxide layers have been employed to protect the photoelectrodes.<sup>14,20,26–30</sup> In particular, titanium dioxide grown by atomic layer deposition (ALD) has been successfully demonstrated as the protection layer on several photocathodes, owing to the chemical stability of titanium dioxide and the high uniformity and conformal nature of the ALD process. For example, Lee et al. demonstrated stable operation of p-InP nanopillars coated with a thin layer of TiO<sub>2</sub>, delivering a high conversion efficiency of ~14% under simulated AM 1.5G illumination, which is among the highest reported to date.<sup>14</sup> Paracchino et al. showed significantly improved stability of Cu<sub>2</sub>O/aluminum-doped ZnO photocathodes with thin TiO<sub>2</sub>

layer by ALD for up to 10 h.<sup>20,21</sup> Seger et al. reported stable operation of n<sup>+</sup>p Si photocathode with TiO<sub>2</sub> protection layer for hydrogen generation for up to 2 weeks.<sup>26,29</sup>

These examples suggest that TiO<sub>2</sub> could in general serve as a protection layer to conduct photogenerated electrons from photocathode materials to the electrolyte and could open up opportunities of utilizing semiconductors that would otherwise be unstable in aqueous electrolyte. However, many of the prior studies have focused on deposition of TiO<sub>2</sub> on a buried semiconductor junction such as Cu<sub>2</sub>O/AZO or n<sup>+</sup>p-Si that provides the photovoltage for water reduction.<sup>20,26</sup> Here, we are interested in understanding the role of TiO<sub>2</sub> deposition directly on p-type photocathodes. Since n-type TiO<sub>2</sub> film has a large valence band offset with most small-band gap p-type semiconductors, it should form a type II junctions and simplify the fabrication process of highly efficient photocathodes.<sup>31</sup>

Here, the effect of TiO<sub>2</sub> thin films on the carrier dynamics, surface recombination velocity, and device performance of InP photocathodes were examined by using photoelectrochemical measurements and impedance spectroscopy. A drastic enhancement of performance for devices coated with a thin optimized TiO<sub>2</sub> layer was observed. Specifically, it is found that in addition to the previously reported protection role,<sup>14,21,26</sup> TiO<sub>2</sub> serves as an effective hole blocking layer on the surface of p-InP while

Received: October 26, 2014

Revised: January 12, 2015

Published: January 14, 2015

allowing the transport of electrons. This favorable surface band-alignment forms a type II heterojunction and leads to surface depletion of holes, thereby drastically reducing the surface recombination velocity of carriers and leading to a 200 mV anodic shift of the onset potential for water reduction. Notably, the p-InP/TiO<sub>2</sub> photocathode with optimal ALD growth process conditions has an onset potential for water reduction of over 800 mV, the highest reported value for InP photocathodes. This represents a major improvement in the PEC cell performance since the onset potential is a key figure of merit for photoelectrodes, similar to the open circuit voltage in solar cells.

## EXPERIMENTAL METHODS

**Fabrication of p-InP/TiO<sub>2</sub> Photocathodes.** The p-InP wafer, with Zn as p-type dopant, was purchased from Wafertech and used as received. A 10 nm Zn/90 nm Au film stack was sputtered on the back of the substrate followed by annealing at 400 °C for 2 min with forming gas flowing to form an ohmic back contact. We used two ALD systems to make conformal TiO<sub>2</sub> coatings. We did not remove the native oxide of InP prior to deposition by, for example, etching in acid. The thickness of the ALD-grown TiO<sub>2</sub> layers was measured using spectroscopic ellipsometry (Jobin Yvon Technology). Titanium dioxide was deposited using a Picosun ALD system at a substrate temperature of 250 °C. Titanium isopropoxide and water were used as Ti and oxygen precursors. The TiO<sub>2</sub> deposition rate was about 0.025 nm/cycle. The thickness of TiO<sub>2</sub> thin film was measured using spectroscopic ellipsometry (Jobin Yvon Technology). The deposition of N-TiO<sub>2</sub> used tetrakis-(dimethylamido)titanium and water as precursors in an Arradance ALD system at 250 °C. The deposition rate is 0.04 nm/cycles. A 2 nm thick platinum layer was sputtered as the hydrogen evolution catalyst on p-InP samples.

**Photoelectrochemical Measurements.** The photoelectrochemical performance of InP/TiO<sub>2</sub> or InP was measured using a three-electrode setup, with a Ag/AgCl reference electrode, and a Pt mesh counter electrode and with InP with and without TiO<sub>2</sub> as the working electrode. The electrolyte was 1.0 M HClO<sub>4</sub> solution purged with forming gas before and during measurement to maintain a well-defined solution potential, with pH value of 0.3. A solar simulator with AM 1.5 filter (Solar Light, model 16S-300-005), the intensity of which was adjusted to 100 mW/cm<sup>2</sup>, was used as light source. The hydrogen gas product was quantified by micro-GC (490 micro GC, Agilent) in 0.1 M HClO<sub>4</sub> solution for every 15 min. The calculated hydrogen amount was calculated based on the passed photogenerated charge at certain time, assuming 100% faradaic efficiency. IPCE (Incident photon to charge conversion efficiency) was measured in a home-built setup, using a 150 W xenon lamp (Newport) coupled with a 1/8 m monochromator (Oriel) as the light source. The intensity of monochromatic light was calibrated with a Si photodiode (Thorlabs FDS100-CAL). The IPCE values were measured at 0.2 V vs RHE. The Mott–Schottky plots of both p-InP wafer and n-TiO<sub>2</sub> on FTO substrate were measured in the dark using the impedance analysis. The electrolyte is 1.0 M HClO<sub>4</sub> solution. The capacitance of the space charge region as a function of applied biases was measured. During the measurement, a sinusoidal voltage perturbation, with amplitude of 5 mV and frequencies of 10k or 20k HZ, was superimposed onto the applied bias. The applied biases were chosen so that the electrode surfaces formed depletion region. The slope of the

MS plot can be used to calculate the carrier density based on the following equation:

$$k = \pm \frac{2}{e\epsilon\epsilon_0 N} \quad (1)$$

in which the negative sign is used to calculate the carrier density of p-type semiconductor, positive sign is used for n-type semiconductor,  $k$  is the slope of MS plot,  $e$  is the elementary charge,  $\epsilon_0$  is the vacuum permittivity,  $\epsilon$  is the dielectric constant of the measured semiconductor ( $\epsilon$  is 12.5 for p-InP and 75 for TiO<sub>2</sub>) and  $N$  is the carrier density. For InP, the energy difference between the valence band edge and Fermi level can be calculated from eq 2:

$$E_f - E_v = \frac{kT}{e} \ln\left(\frac{N_v}{N_A}\right) \quad (2)$$

in which  $k$  is the Boltzmann constant,  $T$  is the temperature,  $e$  is the elementary charge,  $N_v$  is the effective density of state in the valence band, and  $N_A$  is the carrier density of p-InP. Similarly, the energy difference between the conduction band edge and Fermi energy of n-TiO<sub>2</sub> can be calculated from eq 3

$$E_c - E_f = \frac{kT}{e} \ln\left(\frac{N_c}{N_D}\right) \quad (3)$$

in which  $N_c$  is the effective density of states in the conduction band and  $N_D$  is the donor density of TiO<sub>2</sub>. The conduction band edge of p-InP and valence band edge of n-TiO<sub>2</sub> can then be calculated from their optical band gaps.

## RESULTS AND DISCUSSION

Figure 1 compares the photoelectrochemical performance of p-type InP photocathodes with and without TiO<sub>2</sub> coating. A p-type InP (hole concentration of 3–5 × 10<sup>17</sup> cm<sup>-3</sup>) wafer was employed as a photocathode for water splitting because of its 1.35 eV band gap, which is a good match to the solar spectrum and its high achievable energy conversion efficiency.<sup>14,18</sup> A 10 nm thick TiO<sub>2</sub> thin film was deposited on p-InP by ALD using titanium isopropoxide and water as precursors at 250 °C. The thickness and composition of ALD deposited TiO<sub>2</sub> was uniform on the wafer. (Figure S1 and S2, Supporting Information) A 2 nm thick platinum layer was sputtered on both samples as a hydrogen evolution catalyst. Detailed information about the processing and the photoelectrochemical measurement procedures can be found in the Experimental Section. As shown in Figure 1a, the photocurrent onset potential of bare InP, where the water reduction begins, is measured at 0.63 V vs reversible hydrogen electrode (RHE), which is comparable to previous result on bare InP wafers.<sup>15,16</sup> In contrast, InP with a 10 nm TiO<sub>2</sub> thin film can reduce water at a more positive bias of 0.81 V vs RHE, representing a 200 mV anodic shift. Photoelectrochemical measurement of control sample with TiO<sub>2</sub> film deposited on FTO suggests that TiO<sub>2</sub> does not function as light absorber for the improvement. (Figure S3) This result is different from previous result of utilizing TiO<sub>2</sub> to protect n + p Si for water reduction, in which the deposition of TiO<sub>2</sub> did not significantly enhance the photovoltage since the photovoltage is determined by the buried Si homojunction.<sup>26</sup> The photocurrent density of InP/TiO<sub>2</sub> reaches 25.5 mA/cm<sup>2</sup> at the reversible hydrogen potential, which is comparable to the 24 mA/cm<sup>2</sup> obtained on a bare InP electrode. It is noted that the photovoltage achieved by InP/TiO<sub>2</sub> is the highest among InP

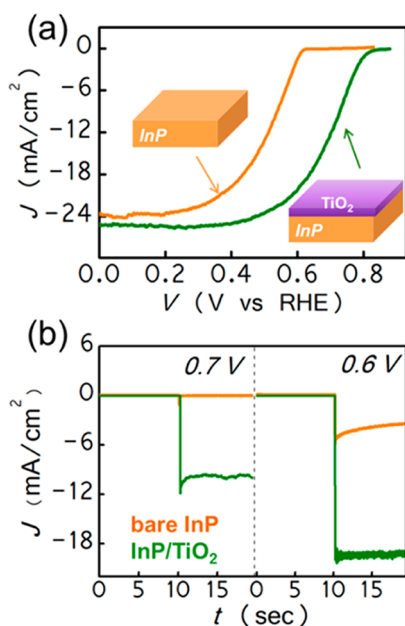


**Figure 1.** Photoelectrochemical characterization performed in 1 M HClO<sub>4</sub> solution of p-InP with and without TiO<sub>2</sub> coating by atomic layer deposition. Pt was used as the hydrogen evolution catalyst in both cases. (a) J-V plots of bare p-InP (orange trace) and p-InP/TiO<sub>2</sub> (green trace) photocathodes measured in 1 M HClO<sub>4</sub> solution under simulated solar light. The intensity was adjusted to 100 mW/cm<sup>2</sup>. (b) Chronoamperometry measurement of bare p-InP and p-InP/TiO<sub>2</sub> at applied biases of 0.7 and 0.6 V vs RHE under chopped light illumination.

photocathodes for water splitting (see comparison in Table S1) and also significantly higher than other photocathodes with comparable band gaps.<sup>11,14,15,19</sup> The photovoltage of InP/TiO<sub>2</sub> photocathode is at least 250 mV higher than p-type Si photocathodes,<sup>11</sup> about 200 mV higher than WSe<sub>2</sub> photocathodes,<sup>19</sup> and about 100 mV higher than p-Cu<sub>2</sub>O photocathode.<sup>23</sup> Photocathodes with such high photovoltage can provide a large portion of the 1.23 V required for the water splitting. The performance advantage of InP/TiO<sub>2</sub> photocathode is further highlighted in Figure 1b, where chronoamperometry measurements of both samples at large positive biases are plotted. Steady photocurrent densities of 9.9 and 19.3 mA/cm<sup>2</sup> were measured at 0.7 and 0.6 V vs RHE on the InP/TiO<sub>2</sub> sample, dramatically higher than the bare InP cathode. Faradaic efficiency measurements performed with the p-InP/TiO<sub>2</sub> photocathodes show that the yield of H<sub>2</sub> is over 95% (Figure S4).

A 200 mV higher photovoltage for water reduction for p-InP with an ALD-deposited TiO<sub>2</sub> layer was measured. However, it was also found that controlling growth chemistry and temperature of TiO<sub>2</sub> by ALD is critical to achieve the high photovoltage. As a comparison, TiO<sub>2</sub> was deposited on p-InP substrates using tetrakis(dimethylamido)titanium and water as precursors at the same temperature. N-TiO<sub>2</sub> denotes the TiO<sub>2</sub> film deposited by tetrakis(dimethylamido)titanium since this precursor contains Ti–N bonds. O-TiO<sub>2</sub> denotes the TiO<sub>2</sub> film deposited using titanium isopropoxide and water. With a 10 nm N-TiO<sub>2</sub> coating, p-InP has a photovoltage of 0.58 V for water reduction, as shown in Figure 2a. The photovoltage is 0.23 V lower than the same InP wafer with TiO<sub>2</sub> deposited using titanium isopropoxide as precursors and even slightly lower than the bare InP photocathodes. The dramatic difference of

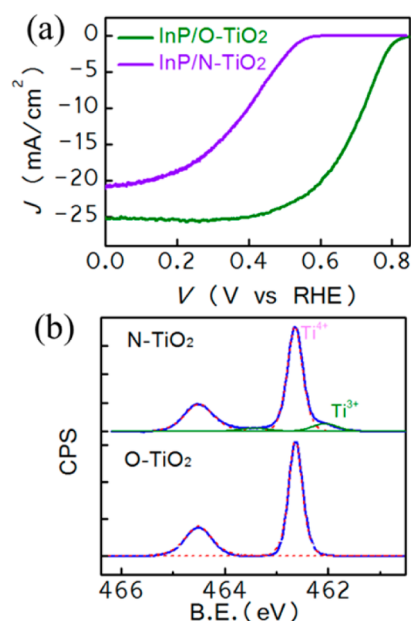


**Figure 2.** Comparison of p-InP/TiO<sub>2</sub> with different growth chemistry. O-TiO<sub>2</sub> denotes the film deposited using titanium isopropoxide discussed previously and N-TiO<sub>2</sub> denotes the film deposited using tetrakis(dimethylamido)titanium. (a) Photoelectrochemical characterization of p-InP with 10 nm TiO<sub>2</sub> grown from different precursors. (b) XPS characterization of N-TiO<sub>2</sub> and O-TiO<sub>2</sub>.

PEC performance of p-InP with various TiO<sub>2</sub> layers can be attributed to the different physical and electronic properties of those TiO<sub>2</sub> films obtained using different process conditions. As revealed by X-ray photoelectron spectroscopy in Figure 2b, the XPS Ti 2p peaks at binding energies of 458.5 and 464.2 eV are assigned to the Ti<sup>4+</sup> valence state in both samples. For N-TiO<sub>2</sub> sample, additional XPS peaks with lower binding energy of 456.8 eV (green fit curve) are assigned to Ti<sup>3+</sup>. The N-TiO<sub>2</sub> film deposited at this temperature is substoichiometric, with reduced Ti<sup>3+</sup> species observed on the surface. In contrast, only Ti<sup>4+</sup> features were observed for the TiO<sub>2</sub> film with titanium isopropoxide as the precursor. Evidently, the Ti<sup>3+</sup> sites enhance electron recombination at the surface compared to both the control wafers and the wafers coated with stoichiometric TiO<sub>2</sub>, which reduces the onset potential. The result clearly highlights the importance of controlling growth chemistry of TiO<sub>2</sub> by ALD to achieve efficient water reduction. The optimal temperature is different depending on the precursor used. To avoid confusion, we only present the result of the stoichiometric TiO<sub>2</sub> film grown using titanium isopropoxide as the precursor in the following discussion.

The onset potential reported here is higher than our previous result of p-InP/TiO<sub>2</sub> photocathodes due to the optimized surface treatment and TiO<sub>2</sub> deposition conditions.<sup>14</sup> Specifically, for the cathodes prepared in this work, we did not remove the native oxide layer on InP prior to ALD of TiO<sub>2</sub>. Through experiments, we found that the devices with an interfacial native oxide layer yield higher photovoltage. This observation is consistent with previous reports highlighting the importance of native oxide for yielding a low trap density for the closely similar InAs/oxide interfaces.<sup>15,32,17,18</sup>

The incident photon to charge conversion efficiency (IPCE) of p-InP devices with and without TiO<sub>2</sub> was also characterized and compared, as plotted in Figure 3. At an applied bias of 0.2 V vs RHE, the IPCE value is 70% to 80% between 800 and 400

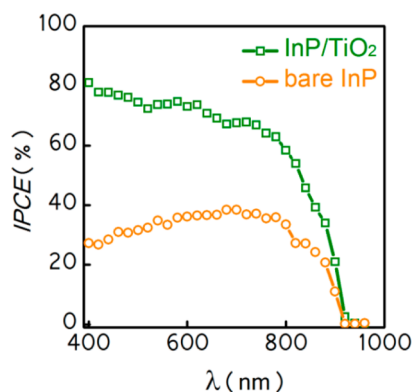


**Figure 3.** Incident photon to charge conversion efficiency (IPCE) of both InP (orange trace) and InP/TiO<sub>2</sub> (green trace) at an applied bias of 0.2 V vs RHE. The electrolyte was 1 M HClO<sub>4</sub> solution.

nm for the sample with TiO<sub>2</sub>, indicating highly efficient photon absorption and charge collection processes in this photocathode. The measurements were performed under low illumination intensity, where surface effects are more prominent. Without TiO<sub>2</sub> coating, the bare InP cathode shows IPCE lower than 30% at the same bias, much lower than the InP/TiO<sub>2</sub> photocathode. We note that the improvement of quantum efficiency by adding TiO<sub>2</sub> layer is distinct at all wavelengths above the band gap. However, there is a distinct improvement in the short wavelength range. Since photons with shorter wavelength are absorbed closer to the surface due to higher absorption coefficient, the conversion efficiency of those photons is therefore more surface sensitive. The IPCE measurement thus suggests that adding TiO<sub>2</sub> layer improves surface properties for minority carrier extraction.

Both J-V and IPCE measurements depict the improved performance of InP photocathodes with TiO<sub>2</sub> coating by ALD. The effect of TiO<sub>2</sub> on InP devices can be attributed to the formation of type II heterojunction with proper band alignment, leading to a reduced surface recombination velocity of photocarriers. It has also been suggested that surface recombination is one of the primary factors contributing to the low photovoltage observed on several III-V semiconductors.<sup>33–35</sup> To explore this effect in more detail, the energy band alignment at the InP/TiO<sub>2</sub> and liquid interfaces was first examined. The flat band potentials and carrier concentrations of a TiO<sub>2</sub> layer (thickness 50 nm) deposited by ALD on an FTO substrate and a p-InP wafer were experimentally obtained by the Mott–Schottky (MS) method, in which the space charge capacitance was measured as a function of applied bias. As shown in Figure 4a, the negative slope of the MS plot shows the p-type nature of the InP wafer. A carrier density of  $3.2 \times 10^{17} \text{ cm}^{-3}$  was extracted from the slope of a linear fit to the MS data, which is in good agreement with the carrier density of  $3\text{--}5 \times 10^{17} \text{ cm}^{-3}$  provided by the supplier. On the other hand, ALD-grown TiO<sub>2</sub>, exhibits a positive slope in the MS plot (Figure 4b), which is indicative of n-type character. An electron density of  $\sim 3.0 \times 10^{18} \text{ cm}^{-3}$  is extracted from the MS slope. Additionally, the flat band potential, which equals the Fermi level of the electrode before reaching equilibrium, of both p-InP and n-TiO<sub>2</sub> can be determined from the MS plots. By extrapolating the  $1/C^2$ -V linear plot to the voltage axis intercept, the flat band potential of InP and TiO<sub>2</sub> were determined to be 0.98 and 0.04 V vs RHE, respectively. The optical band gap of the TiO<sub>2</sub> film grown by ALD was measured

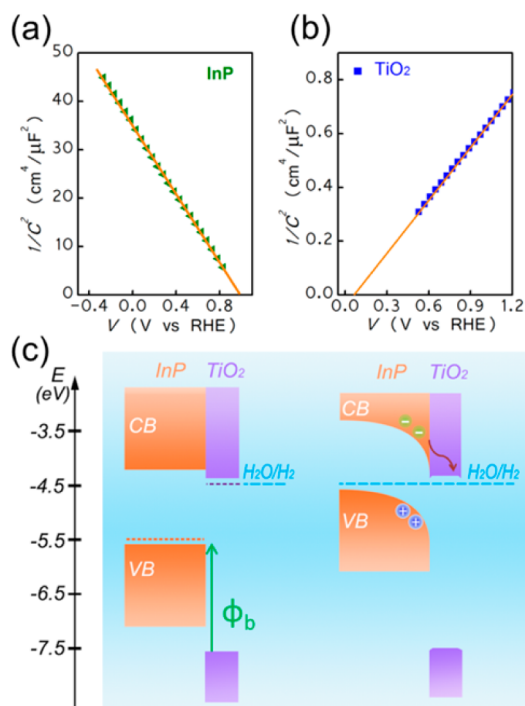


**Figure 4.** Energy diagram of p-InP and TiO<sub>2</sub> in 1 M HClO<sub>4</sub> before and after equilibrium. (a) Mott–Schottky plot measurement for p-InP wafer. (b) Mott–Schottky plot measurement for 50 nm n-TiO<sub>2</sub> on an FTO substrate in 1 M HClO<sub>4</sub> solution. (c) Band alignment of p-InP/TiO<sub>2</sub> in solution based on the Mott–Schottky measurement.

to be 3.1 eV by analysis of a Tauc plot of the optical absorption spectrum. With the measured flat band potentials, carrier densities and the optical band gap, the energy band diagram of InP and TiO<sub>2</sub> in HClO<sub>4</sub> solution before and after equilibrium can be constructed, as shown in Figure 4c. Immediately seen from the energy diagram is that a type II heterojunction is formed between p-InP and n-TiO<sub>2</sub> layer. TiO<sub>2</sub> acts as a selective contact for electron transport for water reduction and as a hole blocking layer. Specifically, the conduction band edges of TiO<sub>2</sub> and InP are aligned such that the transport of photogenerated electrons from InP to the TiO<sub>2</sub> layer is energetically favorable. On the other hand, the large valence band offset between InP and TiO<sub>2</sub>, as shown in Figure 4c, creates a large potential barrier  $\phi_b \sim 1.9 \text{ eV}$  for holes, which leads to electrostatic repulsion of holes from the surface. Reduction of hole concentration at the surface leads to lower surface recombination since for recombination to take place both carrier types must be present. A reduced surface recombination directly leads to a higher IPCE and photovoltage. The hole blocking nature of TiO<sub>2</sub> on p-InP is further proved by the nonohmic I–V measurement of a p-InP/n-TiO<sub>2</sub>/ITO solid state device (Figure S5). It should be noted that similar band-offsets are commonly utilized in high performance Si and III–V solar cells by the use of proper heterojunctions with the same goal of selectively collecting one carrier type while repelling the other.<sup>31</sup> Additionally, reduced surface states density as a result of the amorphous TiO<sub>2</sub> coating is another possibility that could attribute to the lower surface recombination in InP.

In order to further study the effect of TiO<sub>2</sub> on surface recombination, the open circuit voltage ( $V_{oc}$ ) of p-InP with and without TiO<sub>2</sub> as a function of incident light intensity was measured. The  $V_{oc}$  is directly dependent on the magnitude of

nonradiative recombination. As shown in Figure 5, the InP/TiO<sub>2</sub> sample exhibits significantly higher  $V_{oc}$  for all light

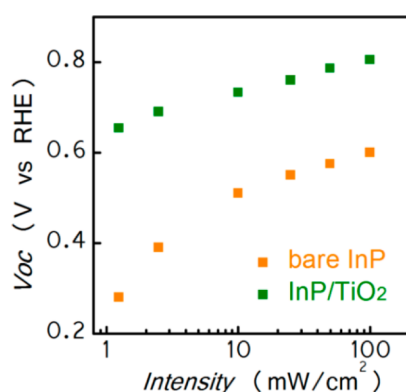


**Figure 5.** Open circuit voltage of both InP (orange trace) and InP/TiO<sub>2</sub> (green trace) as a function of light intensities using simulated sunlight. The light intensity is attenuated using several neutral density filters.

illumination intensities as compared to the bare InP sample. Specifically, under low intensity illumination (e.g.,  $< 3$  mW/cm<sup>2</sup>), the  $V_{oc}$  difference between p-InP photocathode with and without TiO<sub>2</sub> layer is  $\sim 0.37$  V. The  $V_{oc}$  difference is  $\sim 0.2$  V at high illumination intensities ( $> \sim 10$  mW/cm<sup>2</sup>). This behavior is expected since it is known that the  $V_{oc}$  loss due to trap-assisted recombination processes, such as surface recombination, is dependent on the incident light intensity. Specifically, the  $V_{oc}$  loss is less severe at high illumination intensities since a large portion of the trap states are already filled by the photogenerated carriers, thereby reducing the effective non-radiative recombination rate.

Quantitatively, the dependence of  $V_{oc}$  on the illumination intensity is given by the following equation:

$$V_{oc} = \frac{nkT}{q} \ln\left(\frac{I_L}{I_0}\right)$$

where  $I_L$  is the photocurrent density and is proportional to the light intensity,  $I_0$  is the dark current density and  $n$  is the ideality factor. When the ideality factor equals 1, the recombination process is fully governed by radiative recombination. Deviation from the ideal case, such as introduction of nonradiative recombination pathways (e.g., surface recombination), increases the value of  $n$ . The ideality factor of the InP/TiO<sub>2</sub> photocathode is 1.3 from the data in Figure 4, which depicts a near ideal behavior. On the other hand, for the bare InP photocathode, the ideality factor is  $\sim 1.5$  when the light intensity is  $> 10$  mW/cm<sup>2</sup> and 3.2 when the intensity is  $< 3$  mW/cm<sup>2</sup>. These higher values of ideality factor of bare InP electrodes and their light intensity dependence clearly depict the significant nonradiative recombination processes present in bare InP electrodes and supports our claim of reduced surface recombination by TiO<sub>2</sub> coating.

Since surface recombination is one of the dominant processes that limit the photoelectrochemical performance of high-quality crystalline semiconductors, such as InP,<sup>34</sup> the idea of utilizing TiO<sub>2</sub> not just as the protection layer, but also as a hole blocking layer to reduce surface recombination could be generally applicable to improve the photocathode's performance. Utilizing TiO<sub>2</sub> layer as a selective electron contact could also eliminate the need of fabricating solid homojunction for

highly efficient photocathodes.<sup>26</sup> This approach of using stable metal oxides with suitable band alignment to form a heterojunction and reduce surface recombination is also particularly important when employing nanostructured photocathodes,<sup>36,37</sup> which typically exhibits more significant surface recombination owing to the higher surface to volume ratio and is more challenging to fabricate homojunctions.

## CONCLUSIONS

In conclusion, an InP/TiO<sub>2</sub> photocathode for efficient water reduction was demonstrated, with photovoltage over 800 mV vs reversible hydrogen potential. In addition to the previously reported role as the surface protection layer, the thin ALD TiO<sub>2</sub> layer provides the proper surface band-bending for selectively collecting minority electrons while repelling holes. This surface depletion of holes reduces the surface recombination velocity of InP photocathodes. Since surface recombination is a primary efficiency limiting factor in many high-quality crystalline photocathodes, this work of using a TiO<sub>2</sub> layer to reduce surface recombination and enhance photovoltage represents an important advance to achieve efficient solar hydrogen production.

## ASSOCIATED CONTENT

### Supporting Information

Photovoltage comparison of different InP photocathodes, thickness and composition uniformity of TiO<sub>2</sub> film, faradaic efficiency of p-InP/TiO<sub>2</sub> photocathode,  $I$ - $V$  measurement of p-InP/TiO<sub>2</sub>/ITO solid device, and Mott-Schottky plot of p-InP/TiO<sub>2</sub> in electrolyte. This material is available free of charge via the Internet at <http://pubs.acs.org>.

## AUTHOR INFORMATION

### Corresponding Authors

\*(A.J.) E-mail: [ajavey@eecs.berkeley.edu](mailto:ajavey@eecs.berkeley.edu). Telephone: 510-643-7263.

\*(J.A.W.) E-mail: [jwager@lbl.gov](mailto:jwager@lbl.gov). Telephone: 510-486-6715.

### Notes

The authors declare no competing financial interest.

## ACKNOWLEDGMENTS

This material is based upon work performed by the Joint Center for Artificial Photosynthesis, a DOE Energy Innovation Hub, supported through the Office of Science of the U.S. Department of Energy under Award No. DE-SC0004993. A.J. acknowledges support from the WCU program at Suncheon National University.

## REFERENCES

- (1) McConnell, I.; Li, G.; Brudvig, G. W. Energy Conversion in Natural and Artificial Photosynthesis. *Chem. Biol.* **2010**, *17*, 434–447.
- (2) Joya, K. S.; Joya, Y. F.; Ocakoglu, K.; van de Krol, R. Water-Splitting Catalysis and Solar Fuel Devices: Artificial Leaves on the Move. *Angew. Chem., Int. Ed.* **2013**, *52*, 10426–10437.
- (3) Lin, Y.; Yuan, G.; Liu, R.; Zhou, S.; Sheehan, S. W.; Wang, D. Semiconductor Nanostructure-based Photoelectrochemical Water Splitting: a Brief Review. *Chem. Phys. Lett.* **2011**, *507*, 209–215.
- (4) Gratzel, M. Photoelectrochemical cells. *Nature* **2001**, *414*, 338–344.
- (5) Lewis, N. S.; Nocera, D. G. Powering the Planet: Chemical Challenges in Solar Energy Utilization. *Proc. Natl. Acad. Sci. U.S.A.* **2006**, *103*, 15729–15735.

- (6) Kudo, A.; Miseki, Y. Heterogeneous Photocatalyst Materials for Water Splitting. *Chem. Soc. Rev.* **2009**, *38*, 253–278.
- (7) Bensaid, S.; Centi, G.; Garrone, E.; Perathoner, S.; Saracco, G. Towards Artificial Leaves for Solar Hydrogen and Fuels from Carbon Dioxide. *ChemSusChem* **2012**, *5*, 500–521.
- (8) Reece, S. Y.; Hamel, J. A.; Sung, K.; Jarvi, T. D.; Esswein, A. J.; Pijpers, J. J. H.; Nocera, D. G. Wireless Solar Water Splitting Using Silicon-Based Semiconductors and Earth-Abundant Catalysts. *Science* **2011**, *334*, 645–648.
- (9) Khaselev, O.; Turner, J. A. A Monolithic Photovoltaic-Photoelectrochemical Device for Hydrogen Production via Water Splitting. *Science* **1998**, *280*, 425–427.
- (10) Brillet, J.; Yum, J.-H.; Cornuz, M.; Hisatomi, T.; Solarska, R.; Augustynski, J.; Graetzel, M.; Sivula, K. Highly Efficient Water Splitting by a Dual-Absorber Tandem Cell. *Nat. Photonics* **2012**, *6*, 824–828.
- (11) Boettcher, S. W.; Warren, E. L.; Putnam, M. C.; Santori, E. A.; Turner-Evans, D.; Kelzenberg, M. D.; Walter, M. G.; McKone, J. R.; Brunschwig, B. S.; Atwater, H. A.; et al. Photoelectrochemical Hydrogen Evolution Using Si Microwire Arrays. *J. Am. Chem. Soc.* **2011**, *133*, 1216–1219.
- (12) Seger, B.; Laursen, A. B.; Vesborg, P. C. K.; Pedersen, T.; Hansen, O.; Dahl, S.; Chorkendorff, I. Hydrogen Production Using a Molybdenum Sulfide Catalyst on a Titanium-Protected n+p-Silicon Photocathode. *Angew. Chem., Int. Ed.* **2012**, *51*, 9128–9131.
- (13) Sun, K.; Shen, S.; Liang, Y.; Burrows, P. E.; Mao, S. S.; Wang, D. Enabling Silicon for Solar-Fuel Production. *Chem. Rev.* **2014**, *114*, 8662–8719.
- (14) Lee, M. H.; Takei, K.; Zhang, J.; Kapadia, R.; Zheng, M.; Chen, Y.-Z.; Nah, J.; Matthews, T. S.; Chueh, Y.-L.; Ager, J. W.; et al. p-Type InP Nanopillar Photocathodes for Efficient Solar-Driven Hydrogen Production. *Angew. Chem., Int. Ed.* **2012**, *51*, 10760–10764.
- (15) Heller, A.; Vadimsky, R. G. Efficient Solar to Chemical Conversion: 12% Efficient Photoassisted Electrolysis in the [p-type InP(Ru)]/HCl-KCl/Pt(Rh) Cell. *Phys. Rev. Lett.* **1981**, *46*, 1153.
- (16) Aharon-Shalom, E.; Heller, A. Efficient p-InP (Rh-H alloy) and p-InP (Re-H alloy) Hydrogen Evolving Photocathodes. *J. Electrochem. Soc.* **1982**, *129*, 2865–2866.
- (17) Schulte, K. H.; Lewerenz, H. J. Combined Photoelectrochemical Conditioning and Photoelectron Spectroscopy Analysis of InP Photocathodes. I. The Modification Procedure. *Electrochim. Acta* **2002**, *47*, 2633–2638.
- (18) Muñoz, A. G.; Heine, C.; Lublow, M.; Klemm, H. W.; Szabó, N.; Hannappel, T.; Lewerenz, H.-J. Photoelectrochemical Conditioning of MOVPE p-InP Films for Light-Induced Hydrogen Evolution: Chemical, Electronic and Optical Properties. *ECS J. Solid State Sci. Technol.* **2013**, *2*, Q51–Q58.
- (19) McKone, J. R.; Pieterick, A. P.; Gray, H. B.; Lewis, N. S. Hydrogen Evolution from Pt/Ru-Coated p-Type WSe<sub>2</sub> Photocathodes. *J. Am. Chem. Soc.* **2012**, *135*, 223–231.
- (20) Paracchino, A.; Laporte, V.; Sivula, K.; Gratzel, M.; Thimsen, E. Highly Active Oxide Photocathode for Photoelectrochemical Water Reduction. *Nat. Mater.* **2011**, *10*, 456–461.
- (21) Paracchino, A.; Mathews, N.; Hisatomi, T.; Stefik, M.; Tilley, S. D.; Gratzel, M. Ultrathin Films on Copper(I) Oxide Water Splitting Photocathodes: a Study on Performance and Stability. *Energy Environ. Sci.* **2012**, *5*, 8673–8681.
- (22) Siripala, W.; Ivanovskaya, A.; Jaramillo, T. F.; Baeck, S.-H.; McFarland, E. W. A Cu<sub>2</sub>O/TiO<sub>2</sub> Heterojunction Thin Film Cathode for Photoelectrocatalysis. *Solar Energy Mater. Solar Cells* **2003**, *77*, 229–237.
- (23) Dai, P.; Li, W.; Xie, J.; He, Y.; Thorne, J.; McMahon, G.; Zhan, J.; Wang, D. Forming Buried Junctions to Enhance the Photovoltage Generated by Cuprous Oxide in Aqueous Solutions. *Angew. Chem., Int. Ed.* **2014**, *53*, 13493–13497.
- (24) Liu, C.; Sun, J.; Tang, J.; Yang, P. Zn-Doped p-Type Gallium Phosphide Nanowire Photocathodes from a Surfactant-Free Solution Synthesis. *Nano Lett.* **2012**, *12*, 5407–5411.
- (25) Moriya, M.; Minegishi, T.; Kumagai, H.; Katayama, M.; Kubota, J.; Domen, K. Stable Hydrogen Evolution from CdS-Modified CuGaSe<sub>2</sub> Photoelectrode under Visible-Light Irradiation. *J. Am. Chem. Soc.* **2013**, *135*, 3733–3735.
- (26) Seger, B.; Pedersen, T.; Laursen, A. B.; Vesborg, P. C. K.; Hansen, O.; Chorkendorff, I. Using TiO<sub>2</sub> as a Conductive Protective Layer for Photocathodic H<sub>2</sub> Evolution. *J. Am. Chem. Soc.* **2013**, *135*, 1057–1064.
- (27) Lin, Y.; Battaglia, C.; Boccard, M.; Hettick, M.; Yu, Z.; Ballif, C.; Ager, J. W.; Javey, A. Amorphous Si Thin Film Based Photocathodes with High Photovoltage for Efficient Hydrogen Production. *Nano Lett.* **2013**, *13*, 5615–5618.
- (28) Chen, Y. W.; Prange, J. D.; Duhnen, S.; Park, Y.; Gunji, M.; Chidsey, C. E. D.; McIntyre, P. C. Atomic Layer-Deposited Tunnel Oxide Stabilizes Silicon Photoanodes for Water Oxidation. *Nat. Mater.* **2011**, *10*, 6.
- (29) Seger, B.; Tilley, D. S.; Pedersen, T.; Vesborg, P. C. K.; Hansen, O.; Gratzel, M.; Chorkendorff, I. Silicon Protected with Atomic Layer Deposited TiO<sub>2</sub>: Durability Studies of Photocathodic H<sub>2</sub> Evolution. *RSC Adv.* **2013**, *3*, 25902–25907.
- (30) Kohl, P. A.; Frank, S. N.; Bard, A. J. Semiconductor Electrodes: XI. Behavior of n- and p-Type Single Crystal Semiconductors Covered with Thin Films. *J. Electrochem. Soc.* **1977**, *124*, 225–229.
- (31) Yin, X.; Battaglia, C.; Lin, Y.; Chen, K.; Hettick, M.; Zheng, M.; Chen, C.-Y.; Kiriya, D.; Javey, A. 19.2% Efficient InP Heterojunction Solar Cell with Electron-Selective TiO<sub>2</sub> Contact. *ACS Photonics* **2014**, *1*, 1245–1250.
- (32) Takei, K.; Kapadia, R.; Fang, H.; Plis, E.; Krishna, S.; Javey, A. High Quality Interfaces of InAs-on-Insulator Field-Effect Transistors with ZrO<sub>2</sub> Gate Dielectrics. *Appl. Phys. Lett.* **2013**, *102*, 153513.
- (33) Peter, L. M.; Li, J.; Peat, R. Surface Recombination at Semiconductor Electrodes: Part I. Transient and Steady-State Photocurrents. *J. Electroanal. Chem.* **1984**, *165*, 29–40.
- (34) Kelly, J. J.; Memming, R. The Influence of Surface Recombination and Trapping on the Cathodic Photocurrent at p-Type III-V Electrodes. *J. Electrochem. Soc.* **1982**, *129*, 730–738.
- (35) Li, J.; Peter, L. M. Surface Recombination at Semiconductor Electrodes: Part III. Steady-State and Intensity Modulated Photocurrent Response. *J. Electroanal. Chem.* **1985**, *193*, 27–47.
- (36) Cui, Y.; Wang, J.; Plissard, S. R.; Cavalli, A.; Vu, T. T. T.; van Veldhoven, R. P. J.; Gao, L.; Trainor, M.; Verheijen, M. A.; Haverkort, J. E. M.; et al. Efficiency Enhancement of InP Nanowire Solar Cells by Surface Cleaning. *Nano Lett.* **2013**, *13*, 4113–4117.
- (37) Kapadia, R.; Yu, Z.; Wang, H.-H. H.; Zheng, M.; Battaglia, C.; Hettick, M.; Kiriya, D.; Takei, K.; Lobaccaro, P.; Beeman, J. W.; et al. A Direct Thin-Film Path towards Low-Cost Large-Area III-V Photovoltaics. *Sci. Rep.* **2013**, *3*, 2275.